

FABRICATION OF AUTOMOTIVE BRAKE COMPOSITES FROM UNBURNED CARBON

V. M. Malhotra[#], P. S. Valimbe[#], and M. A. Wright^{*}
[#] Department of Physics

^{*} Center for Advanced Friction Studies
Southern Illinois University, Carbondale, IL62901-4401.
E-mail: vmalhotra@physics.siu.edu

KEYWORDS: Unburned Carbon, Coal Combustion By-Products, Friction Materials

ABSTRACT

In pursuit of our goal of finding additional uses for those fly ashes that are rich in unburned carbon, we evaluated how fly ash, bottom ash, sulfate-rich flue gas desulfurization (FGD) scrubber sludge, and unburned carbon affected the frictional properties of composites. We extracted unburned carbon-rich fractions from a fly ash, which was known to have a high carbon content. The unburned carbons were characterized by scanning electron microscopy (SEM), and their oxidative resistance was probed at $30^{\circ}\text{C} < T < 710^{\circ}\text{C}$ using differential scanning calorimetry (DSC) technique. The frictional composites formulated from coal combustion by-products, containing 38-volume percent by-product concentration, were evaluated using Friction Assessment and Screening Test (FAST). Our results suggested that the unburned carbon, being highly porous and resistant to oxidation, had the traits of being an excellent additive for automotive brakes. The composites formed from unburned carbon gave stable frictional behavior and reduced wear and noise.

INTRODUCTION

A substantial portion of the electric power generated in the USA comes from burning coal. However, coal burning by the power plants brings about a huge production of solid residues, mainly fly ash and bottom ash. In an effort to meet the environmental concerns of coal burning, various technologies are employed by electric power utilities, which further add to the solid materials formed, e.g., fluidized bed combustion (FBC) spent bed ash and flue gas desulfurization (FGD) scrubber sludge. It is estimated that about 90 million tons of these solid residues, typically known as coal combustion by-products (CCBs), are produced annually in the USA. Presently, only about 25% of the CCBs generated are utilized [1], with the rest going to landfill or surface impoundments. Most of the CCBs have been largely used in the construction industry, though many additional uses have been proposed [1-4], e.g., ultra-lightweight aggregates for the insulation industry, Portland cement-based FBC mixes, highway and street construction, construction bricks, roofing or paving tiles, pipe construction, artificial reefs for marine wildlife habitat, and aluminum-fly ash composite materials.

In an effort to further mitigate the environmental concerns of coal burning, many utilities have or are installing low- NO_x burner systems [5]. Unfortunately, the fly ash produced by the low- NO_x burner systems has substantially larger unburned carbon in it [5,6]. The higher concentration of unburned carbon in ash stream has a deleterious effect on the utilization of fly ash, especially in the concrete industry. Therefore, intense research is underway by various groups to seek alternative uses of unburned carbon.

The frictional materials used in automobile brake linings are complex composite materials, which generally contain a large number of ingredients, i.e., both organic and inorganic [7]. Typically, brake linings are either organic pads or semi-metallic pads. More than twenty components have been reported for certain brake formulations, though the five major constituents are organic resin as a binder, fibrous reinforcement, filler materials, sliding materials, and friction modifiers. The fillers added into automotive brakes are low cost materials like barytes (BaSO_4), char, and clays. The sliding materials have a hexagonal crystal structure and are incorporated into the frictional materials to alter their lubrication by forming debris on the frictional materials' surface. Asbestos fibers because of their thermal and structural characteristics were frequently used in the recent past as a preferred fibrous support for brake pads. However, they no longer are used due to environmental and health considerations. Slag, mineral, kevlar, or carbon fibers are now used in automotive brakes, depending on the targeted market. Frictional modifiers and abrasives are typically metal oxides. It was felt from our characterization measurements [3,8-9] on CCBs and certain types of carbon extracted from CCBs that the combustion by-products could act as friction modifiers and fillers for automotive brake composites. Moreover, certain fractions of CCBs might help in controlling the thermal properties of brake composites. Therefore, we formed frictional composites from PCC fly ash,

PCC bottom ash, FGD scrubber sludge, and unburned carbon, which was extracted from a high LOI fly ash. These materials' structural, thermal, mechanical, and frictional behaviors were evaluated to probe the suitability of these materials for automotive brake composites.

EXPERIMENTAL TECHNIQUES

The CCBs, i.e., PCC fly ash (Baldwin Unit #3), high LOI PCC fly ash (Southern Illinois Power Co. IL (SIPC)), PCC bottom ash (City Water, Light and Power, Springfield, IL), and sulfate-rich FGD scrubber sludge (City Water, Light and Power, Springfield, IL), samples were obtained from the coal combustion by-product bank maintained in the Mining Engineering department of Southern Illinois University at Carbondale. We used the centrifugation and flotation approach to extract unburned carbon from the high LOI fly ash. Unburned carbon was extracted from two different batches of fly ash obtained from the same power plant, and henceforth, these fractions are called unburned carbon-1 and unburned carbon-2. We blended various CCBs or unburned carbon with polymer binder, slag fibers, and sulfate-rich scrubber sludge to form our composites (see table 1) using a high shear mixer. To minimize the effect of binder on the evaluation of frictional behavior of CCBs, we chose a binder, which is typically used for commercial brake formulations. The blended powders were hot-pressed at 170°C in a 5.72 cm diameter stainless steel die for 1 hour. The hot-pressed composites were further post-cured in air for 8 hours in an oven whose temperature was ramped to 170°C from room temperature at a rate of 3°C/min.

Table 1
Fractions used to form friction composites.

Composite ID	Polymer Binder (volume %)	Slag Fibers (volume %)	Scrubber Sludge (volume %)	By-Product (volume %)
Basic Matrix	45	22	33	
Fly Ash	42	20	30	8 (fly ash)
Bottom Ash	42	20	30	8 (bottom ash)
Carbon-1	42	20	30	8 (unburned carbon-1)
Carbon-2	42	20	30	8 (unburned carbon-2)

Microscopic measurements were undertaken on the as-received fly ash as well as on the unburned carbon fractions by acquiring their SEM microphotographs. The SEM images were obtained using a Hitachi S-570 scanning electron microscope. To record the SEM pictures, a thin layer of fly ash or unburned carbon was sprinkled on a SEM high resolution stub. The samples were then heated at 60°C for 24 hours. These steps were necessary to ensure that ash particles would not detach from the stubs when under electron beam and also would not decompose when under electron bombardment. The fly ash particles were sputter coated with a 40 nm thin layer of gold to reduce sample charging. Generally, the SEM microphotographs were collected using an accelerating voltage of 20 kV. The working distance used was in the range of 8 mm to 12 mm.

The resistance to oxidation of unburned carbon was an important parameter in controlling the oxidative wear of the brake lining formed from CCBs. Therefore, we evaluated the oxidation potential of the unburned carbon by conducting DSC measurements at 30°C < T < 720°C under flowing oxygen conditions. The DSC data were acquired on a Perkin-Elmer DSC7 system, interfaced with a PC 486 computer using a UNIX operating system. The DSC was calibrated for temperature and enthalpy [10,11]. The accuracy in temperature between 30°C and 420°C, based on our calibration procedure, was estimated to be $\pm 1^\circ\text{C}$. The conditions under which the instrument calibration were performed exactly matched the experimental run conditions, namely the scan rate of 20°C/min, oxygen gas purge at 30 psi pressure.

The frictional behavior of our composites, as well as of a commercial automotive brake pad, was obtained with the help of a FAST machine (see Fig. 1). The main elements of the FAST machine are the drive motor and friction cast iron rotor disk, the pivot and load arm, the clamping assembly, and the control valve assembly. FAST test samples of dimensions 12.7 mm X 12.7 mm X 4 mm were placed in contact with a rotor disk. The motor rotated the rotor disk at a constant speed of 875 rpm. A constant frictional force of 0.61 MPa was maintained on the sample as it rotated against the rotor disk throughout the FAST test.

RESULTS AND DISCUSSION

Figure 2 reproduces the SEM microphotograph of the as-received high LOI fly ash sample. As can be seen from this figure, the physical structure of this fly ash had a typical appearance of

PCC fly ashes, i.e., spherical particles of various sizes. Our attempts to locate and probe the physical structure of unburned carbon particles in as-received high LOI fly ash were not successful since no distinct carbon particles could be recognized in Fig. 2. The FTIR

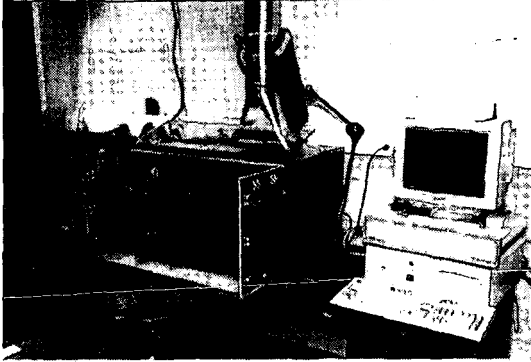
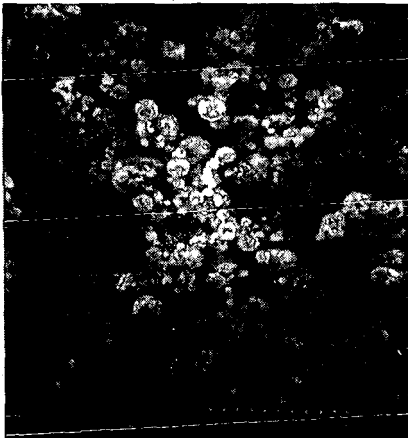


Figure 1. This figure shows the Friction Analysis and Screening Test (FAST) machine used to acquire frictional behavior of our composites.

measurements on as-received fly ash were not helpful either in identifying unburned carbon. Perhaps there were no functional groups in the unburned carbon. It is generally believed that the density of

the unburned carbon particles is lower than the spherical fly ash particles. Therefore, we attempted to separate the high carbon particles from as-received fly ash by centrifugation and flotation. Figure 3 shows the SEM microphotograph of the fraction which floated. It has been suggested that the nature of the unburned carbon in fly ash could be different depending upon the utilities which produce them and the initial structure of coal which undergoes combustion. In fact, Graham et al. [12] proposed that the unburned carbon in fly ashes was actually composed of three petrographically fractions, i.e., inertinite, isotropic coke, and anisotropic coke. The



inertinite fraction in the unburned carbon represents that part of coal which remained unchanged on combustion. The isotropic and anisotropic fractions of unburned

Figure 2. SEM microphotograph of as-received, high LOI PCC fly ash sample. It should be noted that it is difficult to discern the carbon particles in the fly ash.

carbon were those fractions of coal which underwent melting, devolatilization, swelling, and re-solidification during combustion. The isotropic carbon is that carbon which had a high degree of microscopic disorder in its structure, while anisotropic carbon displayed a higher degree of molecular alignment. It is clear from Figure 3 that it is difficult, if not



Figure 3. SEM microphotograph of the particles which were recovered from high LOI fly ash by centrifugation and flotation.

impossible, to distinguish these fractions in the unburned carbon. However, our SEM results did suggest that the unburned carbon in the high LOI fly ash was highly porous and had rough-textured spherical particles. Therefore, unburned carbon particles in frictional composites would facilitate breathing of the material especially under frictional application when the overall brake temperature could be as high as 400°C. The easier escape of the gases, which would be produced at $T > 200^\circ\text{C}$ in frictional materials due to the decomposition of organic fractions, could

reduce the thermal wear of the frictional materials.

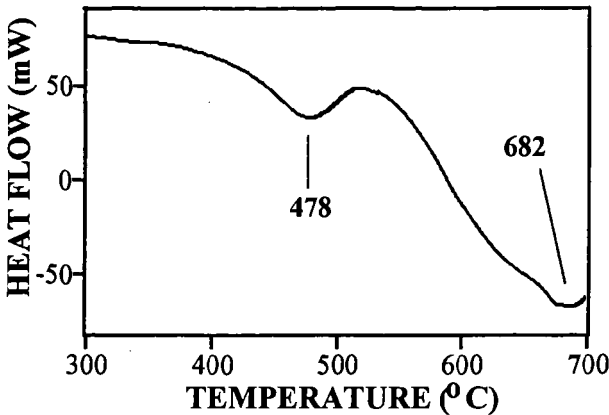
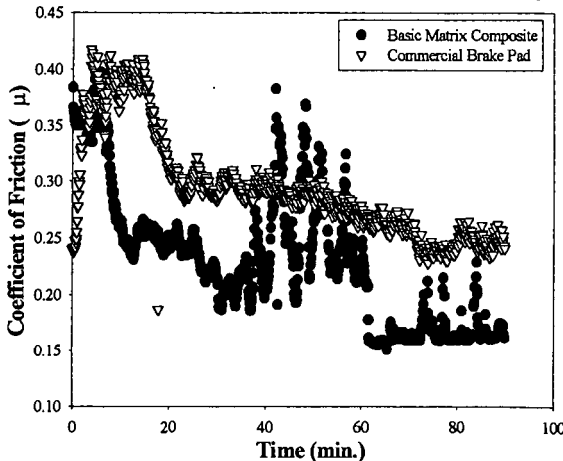


Figure 4: This figure shows the DSC thermograph observed for unburned carbon extracted from high LOI PCC fly ash. The DSC data were collected under flowing oxygen gas conditions.

An important consideration for using unburned carbon in frictional materials would be its resistance to oxidative degradation, especially at temperatures attained by automotive brakes during braking, i.e., $T > 250^{\circ}\text{C}$. Our DSC measurements, conducted under oxygen gas environment, showed no exothermic reactions at $T < 300^{\circ}\text{C}$. In the second batch of runs, we first heated the ash samples to 275°C under nitrogen gas purge environment to ensure the samples were free of water. After soaking the samples at 275°C for 10 minutes, the purge gas was switched to oxygen and the sample's temperature was ramped at the aforementioned heating rate. The typical DSC curve observed from extracted unburned carbon is depicted in Fig. 4. The unburned carbon concentrates, extracted from SIPC fly ash, showed four distinct exothermic reactions, i.e., at 478°C , 610°C , 640°C , and 682°C . The exothermic peaks of 610°C and 640°C overlapped between themselves as well as with the main exothermic peak located at 682°C . At present, it is difficult to assign the exact mechanism of the 478°C exothermic peak. Comparative DSC measurements on other fly ashes suggested that the peak at 478°C originated due to the oxidation of unburned carbon. Since the exothermic reaction of the unburned carbon did not begin until at around 380°C , it appeared that carbon concentrates extracted from fly ashes might be useful additives for automotive brakes.

FAST test results observed for our Basic Matrix composite as well as for a commercial aftermarket automotive brake composite are reproduced in Fig. 5. Generally, unused brake composites show strong variation in the coefficient of friction (μ) in the initial phases of the friction test as material breaks in and its surfaces align with that of the cast iron rotor. Therefore, the variation in μ -value observed in Fig. 5 at time < 10 minutes was attributed to the break in phase. It should be noted that the commercial brake composite μ -value stabilized around 0.3 though it continued to slightly decrease as FAST test time increased. However, this was not the case for our Basic Matrix composite which showed strong variations in the μ -value. The spikes observed in the μ -value could be attributed to the generation of chips from the surface of Basic



Matrix composite. The μ -value decreased to about 0.15 towards the end of the FAST run for Basic Matrix.

Figure 5. FAST test results obtained from a commercial automotive brake and our Basic Matrix composite.

How the incorporation of 8 volume percent of PCC fly ash, PCC bottom ash, or unburned carbon affected the

frictional behavior of our Basic matrix composite is shown in Fig. 6. After the break in period, the μ -value of composites containing fly ash or bottom ash increased to 0.7. As the time of the test increased beyond 60 minutes, the coefficient of friction decreased for both fly ash and

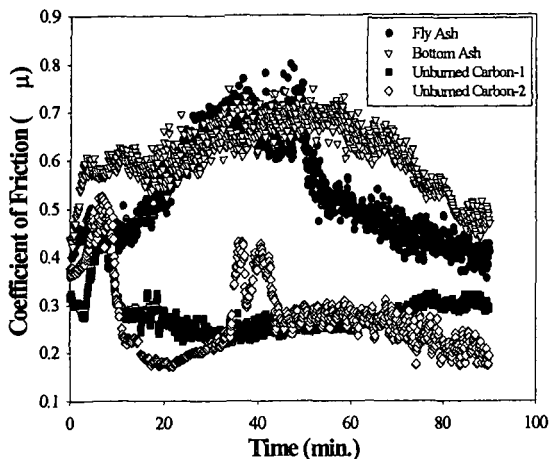


Figure 6. This figure shows how the incorporation of fly ash, bottom ash, or unburned carbon affected the frictional behavior of our composites.

bottom ash containing brake composites. It is important to note that no fade was observed from either of these composites even after 90 minutes of FAST test. The unburned carbon gave much lower μ -value than

those observed from fly ash or bottom ash composite. However, the unburned carbon concentrates not only induced considerable stability in the frictional behavior of our composites but also substantially reduced the noise and wear of the brake composites formulated from CCBs.

CONCLUSIONS

The following was concluded: (a) Our SEM experiments on unburned carbon, extracted from a high LOI PCC fly ash, suggested that the unburned carbon from this ash was highly porous and had rough-textured spherical particles. (b) The unburned carbon was resistant to substantial oxidation at $T < 380^{\circ}\text{C}$, with the major oxidation occurring around 480°C . The porous nature and oxidation resistant traits of unburned carbon made them excellent candidates for automotive brake composites. (c) The incorporation of fly ash, bottom ash, or unburned carbon had a strong effect on the frictional behavior of composites formed from coal combustion by-products. The unburned carbon composites gave desired frictional stability and considerably reduced noise.

ACKNOWLEDGMENTS

This work was supported in the initial stage by the Illinois Clean Coal Institute. Authors also acknowledge the support of this work in part by the Center for Advanced Friction Studies (NSF supported center).

REFERENCES:

1. G. J. McCarthy, F. P. Glasser, D. M. Roy, and R. T. Hemmings, (eds.) *Mater. Res. Soc. Sympos. Proc.* Vol. 113, 1988.
2. L. B. Lee, "Management of FGD Residues: An International Overview.", *Proc. 10th Annual Int. Pittsburgh Coal Conf.*, pp. 561-566, 1993.
3. P. S. Valimbe, V. M. Malhotra, and D. D. Banerjee, D. D., *Am. Chem. Soc. Prep., Div. Fuel Chem.*, 40(4), 776, 1995.
4. J. W. Goodrich-Mahoney, "Coal Combustion By-Products Field Research Program at EPRI: an overview" EPRI (Environmental division), 1994.
5. E. Freeman, Yu-M. Gao, R. Hurt, and E. Suuberg, *Fuel* 76, 761, 1997.
6. R. H. Hurt and J. R. Gibbins, *Fuel* 74, 471, 1995.
7. A. Radisic, P. S. Valimbe, and V. M. Malhotra, *Materials Research Soc. Symp. Series*, 542, 13, 1999.
8. S. P. Kelley, P. S. Valimbe, V. M. Malhotra, and D. D. Banerjee, *Am. Chem. Soc. Prep. Div. Fuel Chem.*, 42(3) 962, 1997.
9. P. S. Valimbe, V. M. Malhotra, and D. D. Banerjee, *Am. Chem. Soc. Prep. Div. Fuel Chem.*, 42(4), 1123, 1997.
10. R. Mu and V. M. Malhotra, *Phys. Rev. B* 44, 4296, 1991.
11. S. Jasty and V. M. Malhotra, *Phys. Rev. B* 45, 1 (1991).
12. U. M. Graham, T. L. Robl, J. Groppo, and C. J. McCormick, "Utilization of Carbons from beneficiated High L.O.I. Fly Ash: Adsorption Characteristics", 1997 Ash Utilization Symposium, Lexington, Kentucky, USA.

RECOVERY AND UTILIZATION OF FLY ASH CARBONS FOR THE DEVELOPMENT OF HIGH-VALUE PRODUCTS

M. Mercedes Maroto-Valer¹, John M. Andrésen¹, Christian A. Andrésen²,
Joel L. Morrison¹ and Harold H. Schobert¹

¹The Pennsylvania State University, The Energy Institute, 405 Academic Activities Building,
University Park, PA 16802-2303, USA

²Norwegian University of Science and Technology, N-7491 Trondheim, Norway

Keywords: Fly ash carbons, activated carbons, carbon artifacts.

The implementation of increasingly stringent Clean Air Act Regulations by the coal utility industry has generally resulted in an increase in the concentration of unburned carbon in coal fly ash due to the installation of low-NO_x burners. Although nowadays the fate of the unburned carbon is mainly disposal, this carbonaceous material is a very attractive precursor for the production of premium carbon products, since it contains >99% carbon and it has gone through a devolatilization process while in the combustor at temperatures well above 1300°C. Accordingly, this work has investigated two potential routes for the generation of premium carbon products from the unburned carbon present in fly ash. The first route focuses on the use of fly ash carbons as precursors for activated carbons by steam activation at 850°C, while the second route concentrates on the utilization of fly ash carbons as a replacement for calcined petroleum coke in the production of carbon artifacts.

INTRODUCTION

The implementation of increasingly stringent Clean Air Act Regulations by the coal utility industry has resulted in an increase in the concentration of unburned carbon in coal combustion fly ash. In 1998, around 5-8 million tons of unburned carbon were disposed, due to the present lack of efficient routes for its utilization. However, the increasingly severe regulations on landfill and the limited access to new disposal sites with the subsequent rise in the cost of disposal, may demand the utility industry to begin offsetting coal combustion with natural gas, or require additional coal cleaning to remove the ash prior to combustion, or simply start utilizing the unburned carbon. The authors have previously conducted extensive studies on the characterization of unburned carbon and showed that its properties are similar to those of conventional precursors for the production of premium carbon materials [1, 2]. Accordingly, this research program focuses on the development of routes for the generation of premium carbon products from the unburned carbon present in fly ash.

The utilization of fly ash carbons can bring enormous economical and environmental benefits to both the coal and utility industries. Although several technologies have been successfully developed to separate the unburned carbon from the fly ash, only a few power plants have installed a beneficiation process on their sites. This is due to the low value of the resultant separated materials, since a ton of fly ash is generally sold for as little as \$10-20, and the unburned carbon is simply disposed or re-routed to the combustor. However, the economics of this process can be greatly enhanced if both separated materials can be used as precursors for value-added products. In fact, this is the case for the unburned carbon, which can be used as an excellent precursor for the generation of premium carbon products, like activated carbons and carbon artifacts. Therefore, the added value generated from the fly ash carbon utilization would clearly offset the cost of the separation process. For instance, the average price for a ton of activated carbon ranges from \$500 up to \$4000, which implies a potential 25-200 fold increase compared to the price of the ash (<\$ 20/tonne). For the case of carbon artifacts, the calcined petroleum coke used for their manufacture usually costs ~ \$ 220-250 / ton.

EXPERIMENTAL

Procurement of fly ash samples The fly ashes were collected from Portland station Unit #2 (Northampton County, PA) with a net capacity of 243 MW and operated by GPU Genco. Samples were collected all the way from the economizer through the hoppers to the stack, amounting to a total of 16 samples. The hoppers were emptied prior to collection in order to obtain fresh ash. The carbon contents of the fly ashes were determined according to the ASTM C311 procedure and the fly ash with the highest carbon concentration was chosen as feedstock for the production of the carbon products.

Activation of fly ash carbons The activation of the samples was carried out in an activation furnace, that consists of a stainless steel tube reactor inside a vertical tube furnace, as previously described [3]. Typically 3 g of sample was held isothermally at 850°C for periods of 60 minutes in flowing steam. The porosity of the samples was characterized conducting N_2 adsorption isotherms at 77K using a Quantachrome adsorption apparatus, Autosorb-1 Model ASiT. The BET surface areas were calculated using the adsorption points at the relative pressures (P/P_0) 0.05 - 0.25. The total pore volume, V_{TOT} , was calculated from the amount of vapor adsorbed at the relative pressure of 0.95. The mesopore (pores 2-50 nm in width) and micropore (pores <2 nm in width) volumes were calculated using the BJH and DR equation, respectively.

Manufacture of carbon artifacts The fly ashes with the highest carbon levels (40-50 wt%) were chosen as feedstocks for the beneficiation step conducted prior to the manufacture of carbon pellets. The beneficiation protocol was performed to be able to elucidate the interactions between the unburned carbon and the pitch, that otherwise may be masked by the high ash concentrations, and included first a flotation separation followed by an acid digestion step using a HF/HCl solution to reduce the inorganic content to ~3 wt%. The carbon pellets were produced from mixtures of this concentrated fly ash carbon (FAC), a petroleum coke (PC) and a coal tar binder pitch (CTBP). The mixtures were heated to ~130°C and pressed into pellets. The absolute densities of the precursors and the pellets were measured by using a Quantachrome MVP-1 Multi Pycnometer with helium as density medium.

RESULTS AND DISCUSSION

Carbon variations between hoppers Fly ash samples were collected from each of the hoppers and Figure 1 shows the configuration and gas flow for the hoppers, and the carbon values of the corresponding fly ashes. The hot-side bins (1-2) present LOI contents of only 10-12%, that become higher for hoppers 5-6 (15 and 19%, respectively) and 9-10 (32 and 36%, respectively) and reach a maximum for the cool-side hoppers 13 and 14 (36 and 50%, respectively). Although this trend also prevails for the train of hoppers 3-7-11-15, it is not so clear, since the LOI values vary only between 14-18%. This "hot-side" and "cool-side" terminology has been adopted from former studies and it is based on characteristics of the respective ashes, where fly ashes from hot-side collectors present characteristics associated with higher temperatures (lower carbon content and larger fly ash sizes) compared to those of their cool-side counterparts [4].

Activation of fly ash carbons Figure 2 shows the N_2 -77K adsorption isotherms for three fly ash carbon samples, designated as FAC-A, FAC-B and FAC-C, and illustrates the inherent porosity of these materials. All the adsorption isotherms are Type II according to the BDDT classification and they are typical for nonporous or macroporous adsorbents, on which unrestricted monolayer-multilayer adsorption can occur [2].

Table 1 lists the BET surface areas (SA) and total pore volume (V_{TOT}) for the precursors. The three samples have surface areas between 30-40 m^2/g . Previous studies conducted by the authors on a range of fly ashes and Density Gradient Centrifugation concentrates have shown that the extensive and rapid devolatilization that coal undergoes in the combustor, seems to promote the generation of meso- and macropores [2]. Pore size distribution studies were also conducted and showed that the pore volume is mainly due to mesopores, with the mesopore volume accounting for over 60% of the total pore volume [2]. The solid yields of the three FAC samples activated for 60 minutes are also listed in Table 1. Despite the low particle size of the FAC samples, the solid yields are relatively high, since the FAC has already undergone devolatilization in the combustor. This makes the UC an attractive precursor for the production of activated carbons, since they present much higher solid yields than conventional precursors, such as wood. FAC-A presents higher solid yields than FAC-B (73% vs. 55%), due to their larger particle size (200 μm vs. 45 μm). Previous studies have shown that the particle size of the precursor strongly affects the solid yields of the resultant activated samples, with higher yields for bigger particle size fractions [5].

Figure 3 shows the N_2 -77K adsorption isotherms for the three steam activated FAC samples. Although the isotherms now look more like Type I, concave to the P/P_0 axis, that are typical for microporous materials, they do not reach a plateau at high relative pressures, indicating the presence of some meso- and macro-porosity. The activated carbons generated from the samples FAC-A and FAC-B present higher adsorption isotherms than that of FAC-C. This is reflected in FAC-A-Act and FAC-B-Act exhibiting surface areas and pore volumes higher than that of FAC-C-Act (332 and 443 m^2/g vs 110 m^2/g , Table 1). This may be due to the lower steam flowrates used for the first two samples, resulting in more favorable conditions for the production of activated carbons. The higher ash content of FAC-C compared to that of FAC-A and FAC-B may also play a detrimental role in the activation of this sample. Further activation studies are being conducted to ascertain the role of the ash in the activation process of the unburned carbon.

Figure 4 compares the meso- and micropore volume for the precursors and the activated samples. As previously described, the inherent porosity of the UC samples is highly mesoporous, with the

mesopore volume accounting for ~ 66% of the total pore volume. The activation process promotes the development of micropores, with the micropore volume now accounting for over 60% of the total. Pore size distribution studies and CO₂ porosity measurements are in progress.

Properties of carbon pellets prepared with fly ash carbons In the preparation of conventional carbon materials, the petroleum coke is used as filler and it is normally separated into at least three different particle size fractions: fine (<200 mesh); intermediate; and coarse (>20 mesh), to obtain improved packing densities. Due to the nature of the combustion process, most fly ashes are milled to the size of the fine fraction or less used for the production of carbon materials. Hence, this study concentrated on the production of carbon pellets, where the fine fraction of petroleum coke was replaced by unburned carbon. Table 2 lists the absolute densities for the carbon pellets produced with the concentrate of fly ash carbon (CFAC), the conventional calcined petroleum coke (PC) and coal tar binder pitch (CTBP). As expected, the density of the carbon pellet A, consisting of 20 wt% coal tar binder pitch and 80 wt% petroleum coke, is slightly lower than that of the petroleum coke itself (1.76 g cm⁻³ vs. 1.89 g cm⁻³). This is due to the lower density of the CTBP (1.25 g cm⁻³), and can be derived from direct calculation of the two fractions (0.2*1.25 g cm⁻³ + 0.8*1.89 g cm⁻³ = 1.76 g cm⁻³). Therefore, for conventional carbon pellets, the CTBP seems to mostly be filling the vacant voids between the PC particles. For pellet B, where all the fine fraction of petroleum coke has been replaced by concentrate unburned carbon, there was a difference between the observed and calculated densities (1.76 g cm⁻³ vs. 1.65 g cm⁻³). This indicates that there is a synergistic filling effect between the unburned carbon and the coal tar binder pitch, that is reflected in a densification of the carbon pellets produced. This could presumably be related to the higher surface area of the concentrated unburned carbon of ~50 m²/g compared to that of 5 m²/g for the calcined petroleum coke, and we are presently conducting further studies to characterize this interaction. These results are very encouraging for further baking of the pellets into artifacts, that is now underway in our laboratory.

CONCLUSIONS

The present work has investigated novel routes for the use of unburned carbon as a high value product. The detailed study of a series of fly ash hoppers has revealed that cool-side bins present the highest LOI values (50%) and therefore they could be suitable hoppers for the collection of high carbon content ashes as precursors for carbon materials. This work has demonstrated the ability of unburned carbon from coal combustion waste to generate activated carbons by steam activation, where after 60 minutes activation time, the unburned carbon samples generated activated carbons with microporous structure and surface areas up to 443 m²/g. Despite the low particle size of the samples investigated, the solid yields are relatively high, since the unburned carbon has already gone through a devolatilization process in the combustor. The activation process can tailor the inherent mesoporosity of these materials into the desired porosity for a specific application. For the case of the carbon artifacts, although the fly ash carbon presents lower density than petroleum coke, the density of the carbon pellets prepared with unburned carbon is comparable to that using only petroleum coke, probably due to a strong interaction between the unburned carbon and the coal tar binder pitch.

ACKNOWLEDGEMENTS

The authors wish to thank the Consortium for Premium Carbon Products from Coal (CPCPC) at The Pennsylvania State University and GPU-Genco/Sithe Energies for financial support.

LITERATURE CITED

1. Maroto-Valer, M.M., Taulbee, D.N. and Hower, J.C., 1999, *Energy & Fuels*, **13**, 947.
2. Maroto-Valer, M.M., Taulbee, D.N. and Hower, J.C., 2000, *Fuel*, In Press.
3. Maroto-Valer, M.M., Andrésen, J.M., and Schobert, H.H., 1999, *Prepr. Am. Chem. Soc. Fuel Division*, **44**, 675.
4. Hower, J.C., Rathbone, R.F., Robl, T.L., Thomas, G.A., Haeberlin, B.O., and Trimble, A.S., 1997, *Waste Management*, **17**, 219.
5. Maroto-Valer, M.M., Taulbee, D.N. and Schobert, H.H., 1999, *Prepr. Am. Chem. Soc. Fuel Division*, **44**, 101.

Table 1. Solid yield, BET surface area and total pore volume for the fly ash carbon samples and their activated counterparts.^a

Sample	Activation time / min	Solid yield / % weight	BET S.A. / m ² /g	V _{total} / cc/g
FAC-A	--	--	40	0.03
FAC-B	--	--	38	0.03
FAC-C	--	--	30	0.02
FAC-A-Act	60	73	332	0.15
FAC-B-Act	60	55	443	0.14
FAC-C-Act	60	79	110	0.04

^a The solid yields and surface areas are expressed in ash free basis.

Table 2. Absolute densities of the carbon pellets prepared.

Pellet	Composition	Density / g cm ⁻³	
A	20% CTBP, 40% intermediate CFAC, 40% fine PC	1.76 ^a	1.76 ^b
B	20% CTBP, 40% intermediate CFAC, 40% fine UC	1.76 ^a	1.65 ^b

^a Density measured by helium pycnometry.

^b Calculated density.

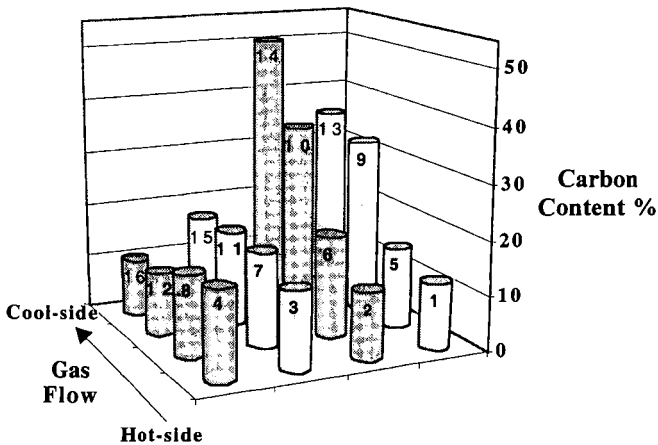


Figure 1. Variation in carbon contents of the fly ashes collected from the different hoppers. The numbers on the bars indicate hopper no.

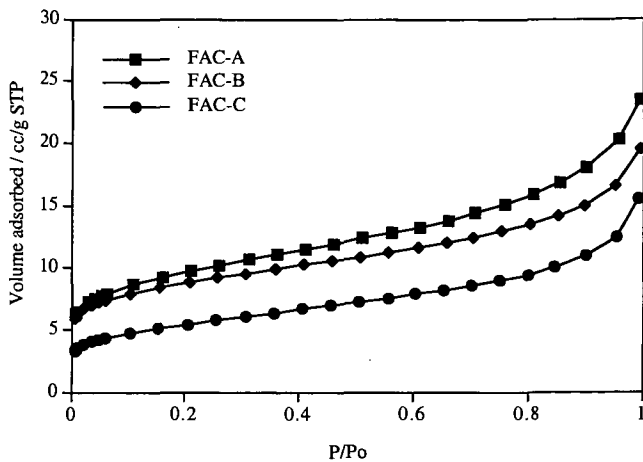


Figure 2. N_2 -77K adsorption isotherms for the fly ash carbons.

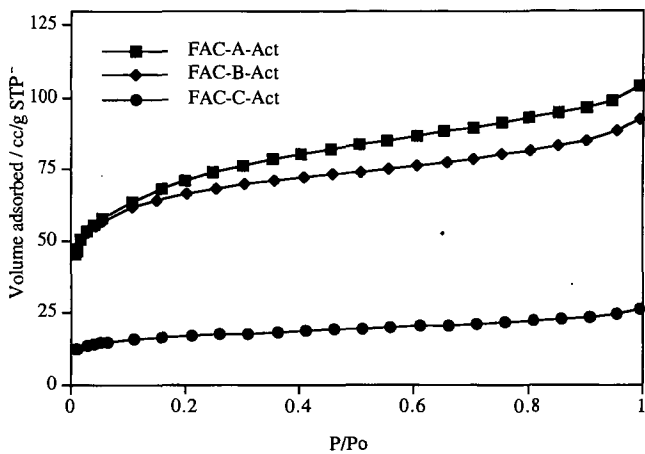


Figure 3. N_2 -77K adsorption isotherms for the activated samples.

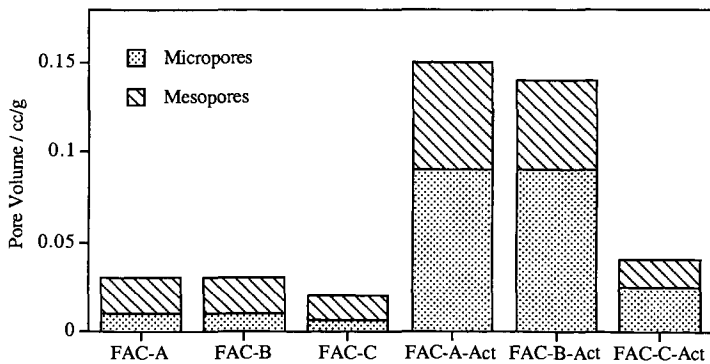


Figure 4. Distribution of the micro- and mesopore volume of the FACs and their activated samples.

Separation and Utilization of Value-Added Products from Combustion Fly Ash

Yee Soong*, McMahan L. Gray, Daniel J. Fauth, Thomas A. Link, J. Richard Jones,
James P. Knoer, Kenneth J. Champagne, Michael R. Schoffstall and Steven S. C. Chuang¹

U.S. Department of Energy, National Energy Technology Laboratory,
P.O. Box 10940, Pittsburgh, PA 15236

¹Chemical Engineering Department, University of Akron, Akron, OH 44325

KEYWORDS: fly ash, separation, and utilization

INTRODUCTION

The utilization of power-plant-derived fly ash has an impact on the cost of power production from coal. The usage has been hindered by recent shifts to low NO_x burners which can increase the carbon content of the ash above the specification (ASTM) for its use in cement applications. Due to the drastic changes in the carbon content in the fly ash, post-combustion beneficiation has been a recent focus of research. Beneficiation processes can generate a valuable unburned organic product and inorganic fly ash product, and these two constituents can be collected and used as commercial products. The unburned organic fraction can be recycled back to the burner as a fuel or used as a catalyst, activated carbon, or catalyst support. The purified inorganic fraction can be utilized as a cement additive or the material for synthesizing molecular sieves. Improved beneficiation and utilization schemes for fly ash can transform it from a waste material, with associated disposal costs, to a valuable product.

Researchers at National Energy Technology Center (NETL) over the last several years have developed a dry triboelectrostatic separation technology for the removal of mineral impurities from pulverized coal and fly ash [1]. In addition, NETL's researchers have extended the agglomeration method utilized for coal beneficiation for the recovery of unburned carbon from fly ash [2]. These techniques have recently been applied to the separation of carbon from fly ash to yield an ash rich product that meet specifications for use in cement applications as well as carbon rich products for other novel applications. The focus of current research is to take the resulting separated fractions, from both dry triboelectrostatic and wet agglomeration processes developed by NETL to explore their potential applications (i.e., activated carbon, molecular sieves, catalytic application, and catalyst supports).

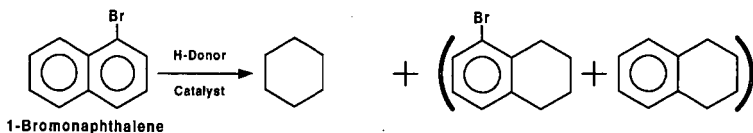
One possible application for fly ash is the synthesis of zeolite products: a process analogous to the formation of natural zeolites from volcanic deposits [3]. Both volcanic ash and fly ash are fine-grained and contain a large amount of aluminosilicate. Amorphous aluminosilicates are the major mineral compounds present in Class F fly ash along with other crystalline minerals, including quartz, mullite, hematite, lime, and feldspars. These chemical and mineralogical features make fly ash a good candidate for zeolite synthesis. In natural conditions, these volcanic deposits may be converted into zeolites by the influence of percolating hot groundwater. This process may take tens to thousands of years under natural conditions. Acceleration of this natural process could result in a cost effective, large scale industrial application for fly ash. Within laboratory conditions, this conversion can be expedited to days. The goal of current research is to establish the optimal conditions for the formation of zeolite products from fly ash.

Carbon materials have been used for a long time in heterogeneous catalysis, because they can act as direct catalysts or, more importantly they can satisfy most of the desirable properties required for a suitable support [4]. Among many types of carbon-supported catalysts (graphite, carbon black, activated carbon, etc.), high surface area activated carbon and carbon black are the carbon materials of choice for most carbon-supported catalysts. Thus, novel applications of carbon derived from fly ash are the focus of current research. Carbon as a catalyst support for the NO_x reduction reaction and carbon as a catalyst for dehalogenation applications are examined.

Farcasiu et al., [5] reported the catalytic activity of carbon black in selective dehydroxylation and dehalogenation reactions under reductive conditions in the presence of a hydrogen donor. Their work has shown that carbon black can catalyze dehydroxylation and dehalogenation reactions of aromatic compounds only in the presence of a hydrogen donor. Within this study, the catalytic reactivity of the carbon concentrates derived from fly ash was examined for hydrodehalogenation of 1-Bromo naphthalene reactions.

EXPERIMENTAL

The details of the dry triboelectrostatic separators and wet agglomeration column were described elsewhere [1,2]. Fly ash (carbon content of 7.74 wt.%) derived from the combustion of a Black Creek Pittsburgh seam coal was utilized for the preparation of carbon concentrates. The 2 wt. % Rh on carbon catalysts were prepared by the impregnation of RhCl_2 over fly ash derived carbon. The NO_x reduction study was conducted in an in-situ infrared cell reactor which was reported elsewhere [6]. Three reaction temperatures, 400, 500 and 650 °C were tested for NO_x reduction activities over the Rh catalysts. The dehalogenation reactions were performed in sealed glass reaction tubes, following the previous described procedures [5]. Ratios of substituted aromatic to solvent to catalyst were 1 : 4 : 0.1. The H-donor solvent was 9,10-dihydrophenanthrene (9,10-DHP). The reaction was conducted at 350 °C for one hour and the products were identified by GC-MS and quantified by GC, using a procedure described elsewhere [5]. The zeolitization process in its simplest form is a relatively straightforward process. Fly ash from Ohio #6A and Meigs Creek coals were mixed with a hydroxide solution in a Teflon reaction vessel and incubated at ambient pressure and various temperatures. At the end of the experiment, mixtures were quenched and the reaction products recovered by filtration.



RESULTS AND DISCUSSIONS

Zeolite synthesis

An initial study using fly ash focused on synthesizing zeolites/zeolitic materials by hydrothermal activation heating. Samples of fly ash were collected by electrostatic precipitation during the combustion of Ohio #6A and Meigs Creek coals. Each sample was sieved through a 100 mesh Tyler screen and calcined at 750°C in air before being analyzed by atomic absorption spectroscopy. SiO_2 and Al_2O_3 were the major components and are the most important reagents for zeolite synthesis. Other crystalline phases identified included mullite ($\text{Al}_6\text{Si}_2\text{O}_{13}$), quartz (SiO_2), hematite (Fe_2O_3), and lime (CaO).

Each fly ash was activated by NaOH and KOH solutions in a closed system. The activations were conducted using a number of Parr digestion bombs equipped with Teflon reactors. Table 1 shows the zeolite synthesis route investigated. Typically, 10.0 g of fly ash was combined with 12.0 g of alkali hydroxide and placed into a covered platinum crucible and slowly heated to 550°C in a muffle furnace. After one hour, the resultant fused fly ash/NaOH mixture was then cooled to ambient temperature and re-ground. About 6 g of fused fly ash/NaOH powder was added to 30 mL of deionized water in a closed Teflon reactor and agitated for 24 hours at room temperature. After aging the solution, the Teflon reactor was then sealed and heated to 100°C without stirring for 48 hrs. The precipitates were filtered, washed repeatedly with deionized water, and dried overnight at 105 °C.

Table 1. Zeolite Synthesis Route

1. Fly Ash - 1.0 part by weight + NaOH or KOH - 1.2 part by weight
2. Treated in air at 550 degrees C for 1 hour
3. Ground fused fly ash to powder
4. Dissolution in distilled water
5. Aging of solution with stirring for 24 hours
6. Heat treatment and precipitation of zeolitic material

Physical synthesis of converted Ohio #6A and Meigs Creek fly ashes into zeolite by utilizing only the supernatant of the dissolved fused powder solutions was completed. Alternate zeolite synthesis path (Table 2) illustrates the systematic approach taken to create a higher surface area material.

Table 2. Alternate Zeolite Synthesis Route

1. Fly ash 1.0 part by weight + NaOH or KOH 1.2 part by weight
2. Treated in air at 550°C for 1 hour, ground to powder, fused fly ash powder
3. Dissolution of fused fly ash powder in distilled water
4. Separation of fused fly ash from supernatant
5. Addition of aluminum hydroxide
6. Aging of supernatant/aluminum hydroxide solution with stirring for 24 hours
7. Heat treatment of supernatant/aluminum hydroxide solution
8. Precipitation of pure zeolite material

Fusion of NaOH (or KOH) with either the Ohio #6A or Meigs Creek fly ash prior to the aging and heat treatment steps produce high amounts of silicates and aluminosilicates, which can be easily dissolved in aqueous solutions. In utilizing the separate •Separation of Fused Fly Ash from Supernatant• step, the formation of zeolite-P is desired. A pre-determined amount of aluminum hydroxide was added after the separation of the mother liquor from the fused fly ash powder sediment. Previous studies by others have shown that Al species may be the controlling parameter in the synthesis. In comparison to the products (NaP-type zeolite) synthesized earlier, the crystalline materials obtained from this alternate synthesis path are significantly lighter in appearance (white in color), due to the absence of unreacted fly ash in solution (green in color).

The specific surface areas of the original Ohio #6A fly ash and its fused NaOH-treated counterpart produced previously were also characterized. The Ohio #6A fly ash was found to have no appreciable surface area, i.e., less than 1 m²/g. Alternatively, the NaOH-treated fly ash/zeolitic material had a specific surface area of 81 m²/g. Surface areas obtained from the KOH-treated fly ash/zeolitic and Meigs Creek samples were very similar (74 m²/g for synthesized zeolite) in comparison to the treated Ohio #6A ash. It is envisioned that the fusion of Meigs Creek ash with KOH will result in zeolite formation at lower temperatures and in less time than with NaOH. Also, the increased effectiveness of KOH should contribute largely to increasing nucleophilicity as the counter cation increases, resulting in a greater dissolution of amorphous aluminosilicates and silicates in the fused fly ash solutions.

Hydrodehalogenation

Carbon concentrates generated from NETL fly ash along with a commercial activated carbon (Black Pearl 2000) were examined for the catalytic activity in hydrodehalogenation of bromine from 1-bromonaphthalene. Five samples received from an oil agglomeration column with carbon concentrations from 37.7 % to 67.3% along with five commercial activated carbons with similar carbon concentrations by diluting with SiO₂ beads were used in the study. The results are illustrated in Figure 1. It appears that the activities of the carbon samples generated by agglomeration and the commercial activated carbon samples are comparable. The increase in carbon concentration correlates with an increase in dehalogenation activity.

NOx reduction

The investigation of unburned carbon material as a catalyst support was conducted in collaboration with the University of Akron. NETL laboratory produced carbon samples from the fly ash derived from the combustion of a Pittsburgh bituminous coal. The University of Akron explored the catalytic properties of the carbon concentrated for NOx reduction.

A 2 wt.% Rh on NETL carbon catalyst was prepared by impregnation of RhCl₃ over the carbon support. The Rh-Carbon catalyst was first reduced in H₂ at 400 °C then exposed to He before exposed to the reactant (1% NO in He). Three reaction temperatures 400, 500 and 650 °C were tested for NOx reduction activities. As illustrated in Figure 2, the immediate production of N₂ (m/e:28), N₂O (m/e:44) and O₂ (m/e:16) after the introduction of NO to the reactor suggest the reactivity of the catalyst. Almost 100 % conversion of NO was observed after exposing to NO at 650 °C. Preliminary results from the University of Akron indicate that the carbon samples from

NETL do show the catalytic activities for NOx reduction.

CONCLUSIONS

Products derived from fly ash were explored for their potential applications as molecular sieves, catalytic applications, and catalyst supports. The fly ash derived zeolite with up to 75% conversion was prepared by the developed zeolite synthesis technique. X-ray diffraction analyses from the prepared zeolite are in accord with that of the natural zeolite-P. The fly ash derived carbon demonstrated good activities for hydrodehalogenation of bromine from 1-bromonaphthalene. Furthermore, the NETL carbon based Rh catalyst showed a good activity for NOx reduction.

REFERENCES

1. Soong, Y., Schoffstall, M. R., Irdi, G. A., and Link, T. A., Proceedings of the 1999 Int. Ash Utilization symposium, pp 548-553, Oct. 18-20, 1999, Lexington, KY.
2. Gray, M. L., Champagne, K. J., Soong, Y., and Finseth, D. H., Proceedings of the 1999 Int. Ash Utilization symposium, pp 603-608, Oct. 18-20, 1999, Lexington, KY.
3. G. Steenburggen and G. G. Hollman, J. of Geochemical Exploration, 62, 305-309 (1998)
4. F. Rodriguez-Reinoso., Carbon Vol. 36, No. 3, 159-175 (1998)
5. M. Farcasiu, S. C. Petrosius, and E. P. Ladner, J of Catalysis 146, 313-316 (1994)
6. Chuang, S. S. C., Brundage, M. A., Balakos, M. W., and Srinivas, G., Applied Spectroscopy, vol. 49, 1152 -1163 (1995)

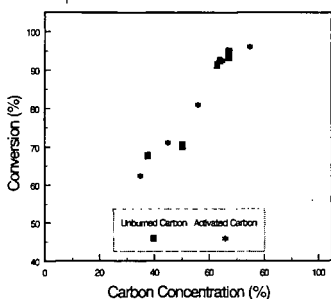


Fig. 1. The Effects of Carbon Concentrates on Dehalogenation Activities

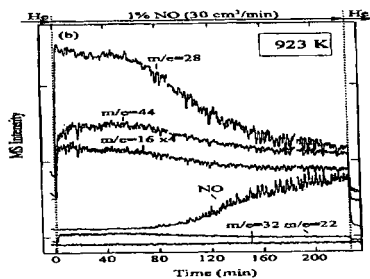


Fig. 2. The reaction of NO over Rh-Carbon catalyst

VALUE ADDED TECHNOLOGY FOR STRIPPER OIL AND GAS WELL BRINES

Robert W. Watson
The Pennsylvania State University
Petroleum and Natural Gas Engineering
125 Hosler
University Park PA 16802

Introduction

The Appalachian Basin oil and gas industry is composed primarily of independent producers operating stripper oil and gas wells in New York, Ohio, Pennsylvania and West Virginia. The wells operated by these independents produce very small quantities of crude oil and natural gas and small volumes of brine. This brine has historically been viewed as a waste product and proper disposal of it is a significant portion of the cost attendant to well operation. In many areas of the United States the brine is disposed of by injecting it into hydrocarbon and/or non-hydrocarbon bearing formations that are both porous and permeable. The Environment Protection Agency (EPA) regulates this subsurface disposal of brine using well injection. EPA categorizes these injection wells to be either Class I or Class II wells. Class I wells according to EPA guidelines¹ are considered to be "technically sophisticated wells that inject large volumes of hazardous and non-hazardous wastes into deep, isolated rock formations that are separated from the lowermost underground source of drinking water (USDW) by many layers of impermeable clay and rock." Class II wells inject fluids (brines) associated with oil and natural gas production. This category of injection wells includes wells that are used for enhanced recovery of oil and gas. The process of enhanced recovery amounts to the injection of fluids such as brine, gas or steam into hydrocarbon bearing zones and thereby recovering oil and gas that would otherwise be unrecoverable. The prerequisite for both Class I and II wells is a formation with adequate permeability and porosity. Permeability is the rock property that defines the rate at which fluid can be injected into a formation. In theory, higher-pressure differentials between the well bore and the formation result in higher injection rates. Limits with respect to pressure differential are imposed by regulations set forth by the EPA. Porosity is a measure of the capacity or voidage space of a rock and along with formation thickness and areal extent define the capacity of the formation. In many areas, there exist no formations that can be used with either Class I or Class II wells and as a consequence alternative methods of disposal are used.

One such alternative method is to treat produced brines in a wastewater treatment facility to remove suspended oils and greases, suspended solids, and heavy metals such as iron prior to discharge into surface water. Commercial brine treatment facilities² of the type located near Franklin, Pennsylvania, and Indiana, Pennsylvania, provide this service to local producers in southern New York and Central Pennsylvania. Transport of the brine to these facilities is by over-the-road tanker. This method of brine disposal is expensive and from an environmental management viewpoint, recovery of this resource is a more desirable alternative. For example, approval has been received to use these brines for stabilizing unpaved rural roads and in conjunction with State Transportation Departments, deicing³. There is no charge to the producer for the disposal of brines used in these applications. Efforts to find other uses for these brines that would result in at least a break-even proposition for producers are underway at The Pennsylvania State University.

Use of Produced Water in Hydrofracturing

Hydrofracturing is a technique of stimulating oil and gas wells. Economides et al.⁴ describes it as consisting of injecting fluid into the formation with such pressure that it induces the parting of the formation. After failure of the rock, the sustained application of the hydraulic pressure extends the fracture outward from the point of failure. Proppants are added to the fracturing fluid to hold open the created fracture after the hydraulic pressure used to generate the fracture is relieved. The fluid used in this process can be very simple or quite complex and the amount of fluid used in the process can vary from a 1,000-gallons to over a 500,000-gallons. Fluids commonly used include water, diesel oil and gases such as Nitrogen and Carbon Dioxide. Material used for propping the fracture include well-sorted sand and spheres composed of ceramic or Bauxite. The amount of proppant used depends on the formation to be fractured. The

capability of the fluid to carry proppant is dependent upon the viscosity of the transport fluid. If the fluid used is water, a guar-derivative such as hydroxypropyl guar (HPG) or carboxymethylhydroxypropyl guar (CMHPG) is added to produce the appropriate viscosity. Other materials added to this fluid can include:

- Biocides – these materials are added to treatment water to control bacterial contamination. There are two types of microorganisms found in water base fluids: aerobic, which consume water base polymers during surface storage, and aerobic, sulfate reducing microorganism that destroy the polymer and produce hydrogen sulfide down hole.
- Gel breakers – used to chemically degrade the guar polymer and thereby reduce its viscosity.
- Surfactants – added to the fluid to reduce surface tension and capillary pressure in pore spaces.

The equipment necessary to hydrofracture a well is significant. Typically, positive displacement pumps capable of moving large volumes of fluid-sand slurries at high pressures are used. These pumps discharge the fluid-sand slurry into a network of high-strength steel piping that is attached to the wellhead. Additional equipment includes trucks to transport and feed the proppant. The capital, operating and maintenance costs associated with this equipment are significant. Consequently, the typical producer purchases the process and materials as a turnkey service.

A gas well drilled in the Appalachian basin penetrates multiple pay zones. These pay zones are Devonian age porous and permeable sandstones. Geologically, these sandstone reservoirs are separated by impermeable shale. The operator typically will select as many as five pay zones in each well for completion. Each pay zone is then isolated and hydrofractured as a separate unit. After drilling to the target depth, casing is run into the well and the annulus space between the casing and drilled hole is filled with cement. The casing adjacent to the zone to be completed is perforated. Perforating is accomplished by lowering into the well a perforator that fires electrically detonated shaped charges from the surface. Clean up of the perforation is accomplished by spearheading the hydrofracturing process with Hydrochloric acid.

The fluid of choice in the Appalachian basin for hydrofracturing is fresh water. Fresh water is used for economic reasons and generally; it is readily available from ponds, streams and/or rivers. Recently however, the Appalachian basin has experienced a regional drought. Independent producers have experimented with using untreated produced brine as a total substitute for fresh water or by mixing the fresh water with brine. Preliminary studies have indicated that it can be used as a replacement for freshwater and the results of the hydrofracturing have been positive.

There are significant questions with respect to the impact of the use of these brines on the productivity of formations. This is particularly true if the brine is used in repeated applications. It is reasonable to expect that the brines will reach a point where their effectiveness will be reduced and their use will result in significant damage to the formation where used.

Mineralogy of Formations

Numerous authors^{5,6,7} have investigated the impact of injected fluids on the clays contained in sandstones. The impact is negative in that it tends to reduce the native permeability of the formation. This reduction in permeability may result from clay swelling and/or mechanical breakdown. For this reason, Potassium Chloride is often added to fresh water before hydrofracturing. This procedure of adding Potassium Chloride was suggested by Black and Hower⁶ and is commonly used in the Appalachian basin.

Clays are negatively charged. The density of negative charges can be measured by determining the number of positive charges required to neutralize the clay crystal. This is known as the cation exchange capacity (CEC) of the clay and is expressed in milliequivalents (ME) for 100-grams of clay. The table below lists the CEC of several clays⁸. The replacement of one cation by another on any clay is governed mainly by the

Cation Exchange Capacity of Selected Clays and Sand

<u>Clay</u>	<u>Range of Cation Exchange Capacity</u>
Smectite	80 to 150
Illite	10 to 40
Kaolinite	3 to 15
Chlorite	10 to 40
Sand (2 to 62 microns)	0.6

Law of mass action and the valence of the cation. Generally, where monovalent and divalent cations are present in the same concentration, the divalent cation will be preferentially attracted to the clay. The physical effect of this phenomenology is that the introduction of freshwater into a clay system will result in permeability damage and a reduction in production. For this reason, Potassium Chloride is added to the fresh water. Among common monovalent cations, potassium has been shown to be more effective than sodium as a method for mitigating clay swelling and damage.

The impact on the clay contained in these formations of using formation brine as the hydrofracturing fluid is not known. In other producing areas, hydrocarbon (oil and gas) and brine from one formation are produced to the surface. The brine is separated from the produced hydrocarbons and often used in drilling and completions effort. In the Appalachian basin, wells penetrating the Middle Devonian sandstones, the hydrocarbons and brines from multiple formations are produced as a commingled stream to the surface through a common well bore. The commingled brine stream is separated at the surface and stored in steel tanks. It is this brine that is used for stimulation purposes.

Hydrofracturing a Middle Devonian Well

The brine used for Hydrofracturing a Middle Devonian well is delivered to the well to be stimulated by over the road tankers. It is pumped into an open-pit that has been lined with an impermeable plastic liner. A centrifugal pump is used to feed the suction side of the positive displacement pumps. The various chemicals and proppants are mixed and added to the brine and displaced into the well at volumetric flow rates of 800-1000 gallons/minute. At the completion of the first stage, the slurry is flowed back into the pit and the process repeated again using the same fluid. This fluid now contains a complex array of chemicals and "solid fines" that are made up of attrited proppants and shale. During each stage, additional chemicals are added and the amount of attrited proppants and shale increases.

Investigation

The purpose of the study is to determine the effect of using these brines in the stimulation process on the ultimate recovery of natural gas from Middle Devonian reservoirs located in the Appalachian basin. There are several questions that need to be answered concerning this procedure. These questions include:

- Given the fact that the mineralogy of each formation is unique, what is the impact of injecting commingled brine into these formations in terms of its impact on the clays contained therein?
- What damage to formation permeability results from the recycling of brine from one stage to the next?
- What damage to formation permeability results from the use of brine that contains micron size "solid fines"?
- What is the impact of this process on ultimate natural gas production and the economics of well development?

To answer these questions, a work plan was developed. The elements contained in the work plan are as follows:

- Five wells will be selected for the analysis. Prior to setting casing in the well bore, sidewall cores of the formations to be hydrofractured will be obtained. The mineralogy of these cores will be determined. Representative brine will be displaced through the cores and the effect on permeability of the brine evaluated.

- The flow-back from each hydrofracture stage will be collected and analyzed to determine changes in the brine given the addition of the chemicals used in hydrofracturing and the presence of solid fines.
- Historical production data will be analyzed to determine any measurable effects of stimulation on ultimate production.

It is expected that this study will be undertaken during the 2000-2001 drilling cycle. A final report is expected during the third quarter of 2001.

Summary

The recent regional drought has created a situation where water necessary for stimulating gas wells was scarce. Independent producers in the Appalachian basin replaced the freshwater used for stimulation with brine that had been produced from existing production wells in the area. The results of this replacement procedure require an assessment to determine whether the procedure impacts ultimate recovery of the natural gas contained in these reservoirs. Moreover, an evaluation of the procedure needs to be undertaken to determine whether changes to it are in order. To accomplish this analysis, a systematic study has been proposed and will be undertaken. Elements of the study include analyses of the rock cores and hydrofracture fluids, and analysis of gas production data.

Bibliography

1. United States Environmental Protection Agency, Office of Ground Water and Drinking Water, "Types of underground injection wells," EPA web site, May, 2000.
2. Adamiak, R.: "Franklin Brine Treatment Plant." Paper presented at the Ohio Oil and Gas Association Technical Meeting, October 13, 1987.
3. Atkinson, J.F., Matsumoto, M.R., Bunn, M.D. and Hodge, D.S.: "Use of Solar Ponds to Reclaim Salt Products from Brine Waters from Oil and Gas Well Operations in New Work," Proceedings of the 1992 International Produced Water Symposium held February 4-7, 1992, in San Diego, California, Edited by James P. Ray and F. Rainer Engelhardt, Plenum Press, New York and London, pp. 535-547 (1992)
4. Economides, M.J., Watters, L.T. and Dunn-Norman, S.: "Petroleum Well Construction, John Wiley & Sons Ltd, West Sussex, England, 1998, p. 473.
5. Weaver, C.E.: "The Clay Petrology of Sediments," *Clays and Clay Minerals*, (1970) V. 18, 165-177.
6. Black, H.N. and Hower, W.F.: "Advantageous Use of Potassium Chloride Water for Fracturing Water Sensitive Formations," API Paper No. 851-39-F presented at Wichita, Kansas, April 3, 1965.
7. Hower, W.F.: "Adsorption of Surfactants by Montmorillonite," *Clays and Clay Minerals*, (1970) V. 18, 97-105.
8. Modern Completion Practices, pp. 9-60 to 9-61, Halliburton Company, (1985).

Adsorption of SO_2 and NO_x by Zeolites Synthesized from Fly Ash, Cement Kiln Dust and Recycled Bottle Glass

Suman Bopaiah and Michael W. Grutzeck
Materials Research Laboratory
The Pennsylvania State University
University Park, PA 16802

Introduction

Natural and synthetic zeolites (molecular sieves) can adsorb SO_2 and NO_x from flue gases. Unfortunately their cost (\$500-\$800 per ton on the East Coast) has deterred their use in this capacity. It has been shown however, that zeolites are relatively easy to synthesize from a variety of natural and man-made materials. The overall objective of the current work was to evaluate the feasibility of using zeolites synthesized from fly ash, cement kiln dust and other recycled materials to adsorb SO_2 and NO_x from flue gases.

Background

Zeolites occur naturally. Normally they are associated with volcanic ash deposits such as those found in Italy, Japan and the West Coast of North America. The ash forms during explosive volcanic eruptions such as the Mount St. Helens eruption a few years ago. The ash that forms during the explosion consists of very fine-grained particles of glass that are rich in alumina and silica. Because of their nature, the ash particles are very reactive. Those that deposit into alkaline lakes will slowly convert into zeolites. In the presence of water and caustic (sodium and/or potassium), the ashes react to form a wide variety of zeolites.

The synthesis of zeolites in a commercial setting is relatively straightforward. Reactive reagents are also used (sodium aluminate, sodium silicate, silica), but in this instance higher temperatures and more concentrated caustic solutions shorten the synthesis process from hundreds of years to a matter of hours or days. If one now begins to think about the potential of using industrial waste products as a source of starting materials for zeolite synthesis, one soon begins to realize that the list can contain a wide variety of materials. For example, aluminosilicate glasses with compositions similar to volcanic ash include fly ash and recycled glass cullet. If one looks for sources of caustics one can add cement kiln dust and a variety of caustic waste streams.

Synthesis procedures are straightforward: add caustic to aluminosilicate glass, allow the mixture to soak to develop precursor gel structures, and then cure at elevated temperatures ranging from 60° to 180°C. Heating the sample causes it to crystallize. The process is well documented for fly ash. More than a dozen papers are available in the literature (1-14). In addition, LaRosa et al. (15,16) and Grutzeck and Siemer (17) found that zeolites Na-P1, X and Y tended to form readily. Adding cement kiln dust (CKD) could alter bulk compositions. The high concentration of potassium in the CKD tended to reduce the need for sodium hydroxide. Recycled bottle glass provided an inexpensive source of sodium silicate (18).

Zeolites normally form on the surfaces of the fly ash particles. Once formed, the zeolites can be used for a wide variety of applications. For example some have been tested for their ability to adsorb ammonia from solution (18). It has been proposed that they be used for wastewater clean up in storm runoff impoundments and sewage treatment plants. Once loaded, they can be used as fertilizer and soil conditioner. These zeolites are also useful for adsorbing gasses such as SO_2 and NO_x from flue gases. Experiments have shown that the proposed technology is viable. Those samples cured at 150°C normally contained analcime while those synthesized at 90°C contained zeolites X, Y and NaP-1. Results suggest that SO_2 removal is 100% efficient until breakthrough and that even after breakthrough some additional adsorption takes place for a significant amount of time. Results also suggest that uptake efficiencies improve in the presence of water vapor. This is an important finding in as much as flue gas contains approximately 10-volume % water vapor. Capacity of zeolites for SO_2 ranged from 10 mg SO_2 /gram to 120 mg SO_2 /gram. These values are within the range reported in the literature for natural and synthetic zeolites.

Experimental Methods

Naturally zeolites were synthesized from fly ash with additions such as ground glass cullet and cement kiln dust. The chemistry is quite forgiving. Phases that form are determined by the bulk chemistry. Variations tend to cause different amounts of the phases to form rather than radically differing phases. The materials are mixed together in the dry state and ball milled with ceramic balls overnight. The resulting powder is then mixed with sodium hydroxide solution, allowed to soak, and then reacted at 90-180°C for a few days. Yields are on the order of 30%

zeolite. The remainder is mullite quench crystals, carbon, iron oxides and unreacted fly ash. The zeolites are filtered and rinsed on filter paper. Then they are ground and dried at 120°C.

Results

Uptake of SO₂ and NO_x was measured using a flow through test apparatus in which a synthetic flue gas containing 2000 ppm SO₂ was passed through a packed bed of various zeolites. The effluent gas was analyzed for SO₂ and NO_x using a Varian 2000 UV/VIS spectrophotometer. The adsorption of SO₂ and NO_x can be followed using their characteristic adsorption band at 284 and 380 nm. Each sample (air-dried, 120°C oven dried, or microwave dried) was tested by first recording a baseline SO₂ concentration in the stack gas by passing the stack gas through the empty adsorption unit (without the zeolite sample). Glass wool was used to seat the sample within the U-tube and so that the finely ground particles of the zeolite would not get entrained in the stack gas exiting the U-tube and entering the spectrophotometer. See Figure 1. As expected, there was little significant adsorption of SO₂ by the glass wool. Second, 1g of zeolite was weighed and placed in the U-tube between two glass wool plugs. The stack gas was passed through the sample at ~4 cc/min and the changes in adsorbance were recorded by the spectrophotometer. The procedure was repeated for each of the three types of dried samples (air dried, oven-dried at 120° C, and microwave dried). Between runs, the system was purged with N₂ gas to establish a SO₂ free baseline. The breakthrough curves were used to theoretically estimate the amount of the SO₂ removed. In as much as SO₂ content is known and total gas passed prior to breakthrough, the amount of SO₂ adsorbed can be calculated. As a check, some of the spent samples were analyzed for total sulfur content and the results obtained were compared to the theoretical calculation of SO₂ removed.

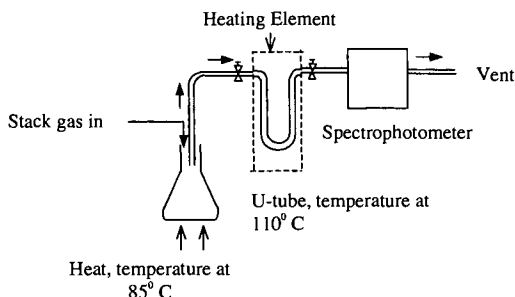


Figure 1. Details of steam generator used to mix water vapor with the simulated gas stream. Tubing running from the tanks to the glass cells was constructed of 5mm stainless steel to insure gas tightness at the ~5psi pressure needed to pass the gas through the packed bed. This set up allowed samples to be tested with or without water vapor present.

Zeolite samples that exhibited a high SO₂ capacity were also tested using the same experimental set-up with the exception that water vapor was introduced into the system. The water vapor source consisted of a 250 ml Pyrex beaker filled with a pre-weighed amount of distilled water kept at ~85°C between the flow meter and the U-tube. See Figure 1. Also, the U-tube sample holder was encased in glass wool and the temperature maintained at 110°C with heating tape to prevent any condensation of the water vapor passing through it. Once again SO₂ as ppm versus time was recorded and as a check, selected samples were chemically analyzed for their total sulfur content before and after they were tested to compare the change in sulfur content. Results are given below.

Adsorption by air-dried samples

Adsorption was first carried out in the absence of water vapor in the influent stack gas. After removing a zeolite sample from its reaction vessel, it was washed with deionized water to remove excess alkali, and then dried in room temperature air. One gram of the zeolite was weighed out and finely ground with a mortar and pestle and placed in the sample holder between plugs of glass wool. Initial tests were conducted with the background SO₂ concentration being

recorded for reference. The sample of zeolite depicted in Figure 2 showed a reasonable amount of SO₂ uptake. The break-through curve exhibited a maximum (100% SO₂) uptake for ~25 minutes.

In the next test, before introducing the sample, water vapor from the Erlenmeyer flask maintained at 85°C (Figure 1) was mixed with the gas and allowed to flow through the system. In this case, a dramatic increase in the adsorption capacity of the zeolite was seen due to the presence of water vapor. See Figure 2. Complete removal of SO₂ molecules from the influent stack gas and steam occurred for about 86 minutes after which SO₂ removal continued to occur, though 100% removal was not seen beyond that point. Sulfur analyses of the air sample tested in the presence of water vapor showed SO₂ concentrations of 10 wt% which is roughly in agreement with SO₂ uptake calculated

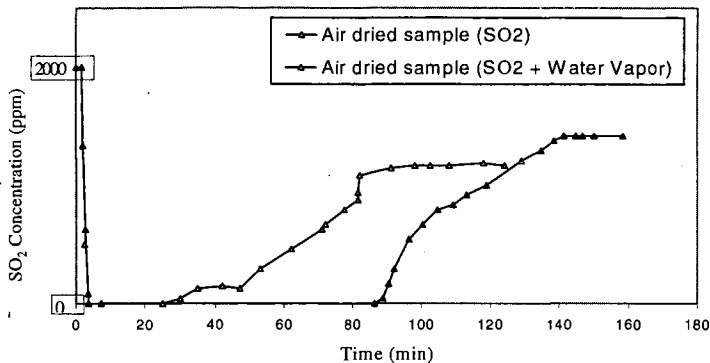


Figure 2. Breakthrough adsorption curves of air-dried zeolite sample (unknown phase) made with Class F+C fly ash, cement kiln dust and silica fume and then used to treat a simulated stack gas of (a) 2000 ppm SO₂ (~25 min to breakthrough) and (b) 2000 ppm SO₂ plus saturated water vapor (~86 min to breakthrough). Flow

from the graph in Figure 2.

Adsorption by samples dried at 120°C

Similar tests were carried out with complimentary samples that were dried at 120 °C overnight. These samples (same as above) also showed an increase in adsorption in the presence of saturated water vapor. The sample showed complete adsorption in the absence of water vapor for 8 minutes but this value increased in the presence of water vapor to 23 minutes as shown in Figure 3. This again shows the increase in SO₂ uptake in the presence of water vapor. Sulfur analyses of the oven dried sample tested in the presence of water vapor showed SO₂ concentrations of 6 wt%. Surprisingly, the degree of pre-drying had a negative impact on the adsorption capacity of the zeolite.

Discussion

In the case of the air-dried samples, the dramatic increase in adsorption in the presence of water vapor is thought to occur due to the dissolution of the SO₂ molecules in the water molecules adsorbed on the surface of the zeolite sample. Subsequently, oxidation of the SO₂ molecules to sulfate and sulfite might have occurred at the temperature of 120 °C, which was constantly maintained. This oxidation of SO₂ molecules is known to be temperature sensitive as previously observed by Tsuchai et al. (19) using an absorbent prepared by coal fly ash, calcium oxide and calcium sulfate. In

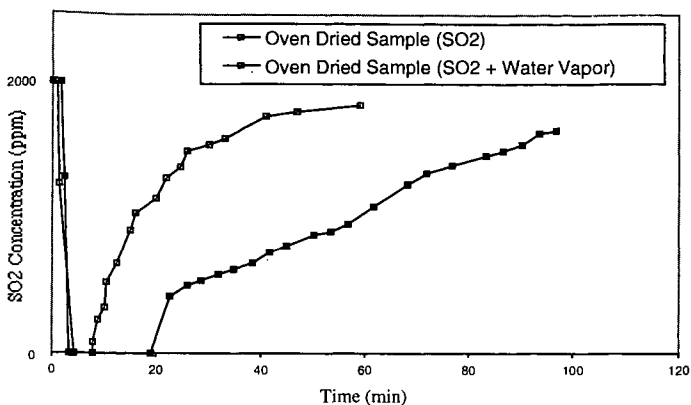


Figure 3. Breakthrough adsorption curves of same oven-dried zeolite sample with simulated stack gas of (a) 2000 ppm SO₂ (~8 min to break-through) and (b) 2000 ppm SO₂ and saturated water vapor (~23 min to breakthrough). Flow rate ~4 cc/s. Calculated uptake of 23 minute breakthrough sample=3 wt%.

this study, Tsuchai et al. proposed that a monolayer of water is formed at the surface of the absorbent in the presence of relative humidity. Above the monolayer, SO₂ dissolves in the layer while below the layer, SO₂ forms calcium sulfate due to the presence of NO and the chemical composition of the absorbent used.

In the case of the oven-dried samples, possibly, the structure of the zeolite might have undergone changes due to the overnight heating at 120°C. Though this might have occurred, an increase in adsorption was still seen in the case of the sample subjected to water vapor. This could be due to the sulfur dioxide oxidation occurring mainly at the surface of the sample rather than deep in the interior cages and channels as for the air dried sample.

Summary

A graphic representation of SO₂ adsorption results in milligrams SO₂ adsorbed per gram of tested zeolitic material is given in Figure 4. The results are typical of those obtained for air and microwave dried zeolites synthesized at 100°C. One sample (NaP-1) was regenerated by heating it in air. It was regeneratable, but less effective at adsorbing SO₂ the second time around. As seen in Figure 4, zeolites used to extract SO₂ from the simulated stack gas in the presence of water vapor could adsorb nearly 120 mg of SO₂/gram of sample. Also, surprisingly enough, zeolite samples that initially contained water (those that were air dried versus those that were dried at 110°C) tended to adsorb more SO₂ than their "drier" counterparts. Note, however, that microwave drying (MW in table) tended to increase SO₂ capacities for identical samples (oven versus microwave dried) of clinoptilolite and phillipsite run in a non-water vapor containing atmosphere. The effect of microwave drying is still being investigated, as data seem to be contradictory at this point in time.

One interesting observation was the fact that these fly ash-based zeolites were also able to adsorb NO₂ from a gas mixture containing 2000 ppm NO₂ (balance N₂). The sample in question was reacted at 90°C for 56 days. It was non-crystalline (X-ray amorphous) which is notable in as much as adsorption is usually correlated with crystallinity. Perhaps, short-range order is enough to capture certain gases. It was able to capture 88 mg NO₂/gram of zeolite. It is suggested that this property could turn out to be even more important than the zeolite's SO₂ adsorption capacity.

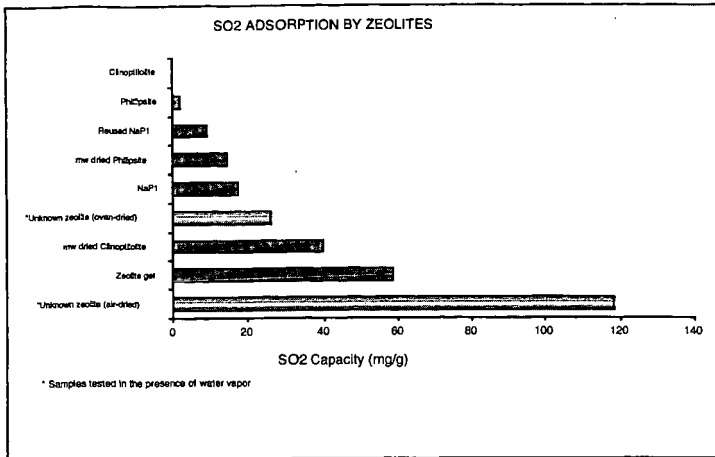


Figure 7. Relative capacities for SO₂ of samples tested with and without water vapor. Note that some of these are "dry" values and adsorption is normally two or three times higher in the presence of water vapor.

References

1. Henmi, T. *Soil Sci. Plant Nutr.* **1987**, 33, 517-521.
2. Mondragon, F.; Rincon, F.; Sierra, L.; Escobar, J.; Ramirez, J.; Fernandez, J. *Fuel* **1990**, 69, 263-266.
3. Shigemoto, N.; Shirakami, K.; Hirano, S.; Hayashi, H. *Nippon Kagaku Kaishi* **1992**, 484-92.
4. Shigemoto, N.; Hayashi, H.; Miyaura, K. *J. Mat. Sci.* **1993**, 28, 4781-86.
5. Chang, H.-L.; Shih, W.-H. In *Environmental Issues and Waste Management Technologies V*; Jain, V; Palmer, R., Eds.; Ceramic Transactions 61; Amer. Ceram. Soc.: Westerville, OH 1995; pp. 81-88.
6. Lin, C.-F.; Hsi, H.-C. *Environ. Sci. Tech.* **1995**, 29, 1109-17.
7. Park, M.; Choi, J. *Clay Sci.* **1995**, 9, 219-229.
8. Querol, X.; Alastuey, A.; Fernandez-Turiel, J.L.; Lopez-Soler, A. *Fuel* **1995**, 74, 1226-31.
9. Shigemoto, N.; Sugiyama, S.; Hayashi, H.; Miyaura, K. *J. Mat. Sci.* **1995**, 30, 5777-83.
10. Shih, W.-H.; Chang, H.-L.; Shen, Z. *Mat. Res. Soc. Symp. Proc. Vol. 371*; Materials Res. Soc: Pittsburgh 1995; pp 39-44.
11. Singer, A.; Bergaut, V. *Environ. Sci. Technol.* **1995**, 29, 1748-53.
12. Amrhein, C.; Haghnia, G.H.; Kim, T.S.; Mosher, P.A.; Gagajena, R.C.; Amanios, T.; de La Torre, L. *Environ. Sci. Tech.* **1996**, 30, 735-740.
13. Suyarna, Y.; Katayama, K.; Meguro, M. *Chem. Soc. Japan* **1996**, 136-40.
14. Querol, X.; Alastuey, A.; Lopez-Soler, A.; Plana, F.; Andres, J. M.; Juan, R.; Ferrer, P.; Ruiz, C.R. *Environ. Sci. Tech.* **1997**, 31, 2527-13.
15. LaRosa, J.; Kwan, S.; Grutzeck, M.W. *J. Amer. Ceram. Soc.* **1992**, 75, 1574.
16. LaRosa, J.; Kwan, S.; Grutzeck, M.W. In *Mat. Res. Soc. Symp. Proc. 245*; Mat. Res. Soc.: Pittsburgh, 1992; pp. 211-16.
17. Grutzeck, M.W.; Siemer, D.D. *J. Amer. Ceram. Soc.* **1997**, 80, 2449-53.
18. Grutzeck, M.W. and J. A. Marks, *J. Environ. Sci. Eng.* **1999**, 33, 312-317.
19. Tsuchiai, H., T. Ishizuka, H. Nakamura, T. Ueno, H. Hattori, *Ind. Eng. Chem. Res.* **1996**, 35, 851-855.

Acknowledgements

Support by the FETC Grant Number DE-FG22-96PC96210 is gratefully acknowledged.

SYNTHESIS AND CHARACTERIZATION OF A NOVEL MULTIFUNCTIONAL CARBON MOLECULAR SIEVE

Wei XING and Zi-Feng YAN*

State Key Laboratory for Heavy Oil Processing,
University of Petroleum, Dongying 257061, P R China

ABSTRACT Carbon molecular sieves were prepared from petroleum coke by chemical activation. The effects of activation temperature, holding time, preliminary treatments and activated agent ratio on surface area, pore structure of the carbon molecular sieves produced in our lab were investigated. The specific surface area and average pore size of the carbon are obviously increased with increasing use of activator and rise of activating temperature. The rate of elevating temperature is not specifically limited. But the heat-retaining time has much influence on the performance of the activated carbon. Suitable holding time may lead to high degree of activation, with result of increase in pore diameter of micropore and mesopore. But too long holding time can destroy pore structure and result in decrease of specific area. In addition, the effects of coke pre-oxidation on activating results were also investigated. Coke pre-oxidation leads to a remarkable decrease of mesopore volume. The carbon molecular sieves prepared in our lab are about 3000 m²/g in BET specific area. Diffraction peaks in XRD patterns indicate the generation of a new crystalline phase of carbon. The prepared carbon molecular sieves with extremely high specific area and uniform micropore distribution are ideal materials for natural gas adsorption storage as vehicular fuel. Carbon molecular sieves differing in BET surface area were used to evaluate the natural gas storage capacity on them at different pressures by two-vessel volumetric method at 293 K and up to 5.0 MPa. In addition, this kind of carbon molecular sieve can also be used as microwave absorbent and PSA adsorbent for gas separation.

KEYWORDS Carbon molecular sieve, natural gas absorption, chemical activation

1. INTRODUCTION

Petroleum coke is a material of low volatility produced during the refining of crude oil and generally comprises carbonaceous material including elemental carbon, as well as relatively heavy hydrocarbon products including straight- and branched-chain saturated and unsaturated hydrocarbons, cyclic and polycyclic saturated and unsaturated hydrocarbons, whether unsubstituted or substituted with acyl, cyano, sulfur, or halogen constituents, and organometallic compounds. It is abundant and cheap, being widely used as fuels and for the production of graphite electrodes in electric furnace smelting.

A new value-added carbon product, a novel multifunctional carbon molecular sieve, is developed from petroleum coke, which can be widely used as natural gas adsorbent, microwave absorbent and, after pore structure modification, PSA adsorbent for gas separation.

2. EXPERIMENTAL

2.1 Preparation of Carbon Molecular Sieve

Carbon molecular sieves were prepared from petroleum coke (manufactured by ShengLi-Refinery) which mainly consists of carbon atoms, more than 90%, with minor other atoms such as S, N and heavy metals. The raw material, hard, compact and non-porous, was grounded and sieved from 100 ~ 200 mesh. The activator is prepared by mixing, slurring and stabilizing an alkali metal hydroxide or oxide with other transition metal chlorides or nitrates. Petroleum coke powder was chemically activated using alkali metal hydroxides or oxides as the reagent, and acetone or ethanol as the surfactant. Activated agent, acetone and water were added in specific amounts to petroleum coke. The mixture was stirred homogeneously, giving slurry. The activation of petroleum coke was then carried out in a parallel stainless steel reactor at a certain temperature. The effects of activation temperature, holding time, preliminary treatments and activated agent ratio on surface area, pore structure, and methane storage capacity of the carbon produced in our laboratory were investigated. After activation, the sample was submerged in deionized water, filtered and rinsed again in deionized water to remove any activator derivatives.

In addition, the pre-oxidation of the coke powder on activating results was also investigated. The coke powder was oxidized in air at 473K for 24 hours prior to activation.

* To whom correspondence should be addressed-mail: zfyancat@sunctr.hdpu.edu.cn

2.2 Characterization of Carbon Molecular Sieve

The surface properties such as surface area, average pore diameter and pore volume were determined using an automatic ASAP2010 apparatus (Micromeritics) by N_2 adsorption at 77.5K. The total pore volume, V_t , is derived from the amount of absorption at a pressure relatively close to unity, given that the pores were totally filled with the liquid adsorbate. The mesopore distribution curve is obtained from the absorption branch of the N_2 isotherm by BJH method. The micropore distribution is calculated from the gas absorption using the Horvath-Kawazoe equation, with relatively pressure (P/P_0) below 0.01. Adsorption isotherms of CH_4 have also measured by two-vessel volumetric method in a high-pressure range (0–5.0MPa) at ambient temperature.

A BDX-3200 X-ray powder diffractometer, manufactured by Peking University Instrument Factory, was used to identify the crystal form of carbon molecular sieve. Anode Cu $K\alpha$ (40kV, 20mA) was employed as the X-ray radiation source, covering 2θ between 20° and 120° . The XRD patterns were monitored and processed by a computer.

The surface morphology of carbon adsorbents was observed using scanning electron microscopy (JEM 5410LV, JEOL Technologies) with the accelerating voltage of 25kV. The surface elemental composition of carbon molecular sieve was determined by energy distribution spectrum using X-ray microanalysis (ISIS, Oxford Instrument).

3. RESULTS AND DISCUSSION

3.1 Pore Structure Variation of Carbon Molecular Sieve

(1) Effect of Activated Agent Ratio on Structure Variation of Carbon Molecular Sieve

Carbon molecular sieves were prepared by chemical activation using various amounts of activated agent. A quantitative comparison of the variation of the textural structure, mesopore and micropore distribution of carbon molecular sieves is given in Table 1.

The results show that specific surface area, average pore size, average micropore size and pore volume in different size range is obviously increased with increasing use of activator. It means that the amount of activator used determine the depth of activation. The more activator is used, the more micropores are developed. It can be seen from Table 1 and Figure 1 that the volume of pore range from 7 to 30\AA , which is believed to play a role for natural gas adsorption in relatively low pressure, takes up about 90% in the total pore volume. The adsorption isotherms of all carbon molecular sieves shown in Figure 1(b) belong to typical type I isotherm, which also indicates that carbon molecular sieve is a microporous carbon-based material.

(2) Effect of Activating Temperature on Structure Variation of Carbon Molecular Sieve

Petroleum coke was activated at different temperature, which resulted in the variation of pore structure for carbon molecular sieve. Table 2 shows that specific surface area, pore diameter and pore volume all change to be larger with the rise of activating temperature. Obviously, the mesopore ($>20\text{\AA}$) volume increases more substantially than the micropore volume. It should be also noted that a shorter period is demanded for activation at high temperature. Excessively long period of heat retaining at high temperature may be responsible for the deviation of activation results at 1173K. It may destroy micropore structure and result in the decrease of specific area.

(3) Effect of coke preoxidation on Structure Variation of Carbon Molecular Sieve

Petroleum coke was preoxidized at 573K for 24 hours in air prior to activation. Table 3 shows the variation of pore structure on carbon molecular sieves caused by preoxidation. We can draw a conclusion from Table 3 that mesopore ($>20\text{\AA}$) volume decreases remarkably due to preoxidation. The decline of mesopore volume range from 20\AA to 30\AA may be disadvantageous for natural gas absorptive storage. However, the decrease of mesopore ($>20\text{\AA}$) volume results in increase of density for carbon molecular sieves, which is meaningful for natural gas storage.^[1] More importantly, it provides a possible way to produce carbon molecular sieve with uniform micropore-size distribution.

3.2 XRD Characterization

Natural gas is absorbed in the micropores that is close related to the crystal structure of carbon molecular sieve. Understanding the crystal structure of carbon molecular sieve is instructive not only for structural optimization of adsorbents prepared, but also for the accurate evaluation BET, porosity, etc., of adsorbents.

The major crystalline phases of carbon molecular sieve were examined by XRD and the spectra were presented in Figure 2. There are 4 sharp peaks visible, which can be indexed as (100, 111, 200, 210) of a primitive cubic unit cell with a unit cell length of 2.026\AA . Assuming a disordered rhombohedral (hexagonal) cell, this calculates to $a = 1.43$ and $c = 3.51\text{\AA}$ which is comparable to the distances in graphite, 3.35\AA , within and perpendicular to the layers. Although

how the carbon crystal lattice arranges to form this centralized distribution of micropore is not known exactly, it is a really interesting point worth further studying. It may be the fundamental to understand the nature of gas absorptive storage on carbon.

3.3 SEM and EDX Analysis

The microscopic appearance observation of the carbon was conducted using scanning electron microscopy. The micrographs of absorbents, derived from raw coke and preoxidized coke respectively, are illustrated in Figure 3, from which the porous structure of absorbents is clearly imaged. The markedly different surface morphology between these two absorbents indicates various reacting processes during activation. The pore shapes of absorbents prepared from raw coke look randomly, while the pore shapes prepared from preoxidized coke are circular universally. Although the formation mechanism of these circular pores is not known exactly, it is believed to be close relative with retarding the formation of mesopore, which is reflected in Table 3. After preoxidation at 473K in air for 24 hours, surface oxides generated on the surface of the coke. During activation, these surface oxides removed primarily to form rudimentary pores, which is reckoned to be in favor of subsequent activation.

The surface elemental composition of the absorbents was also characterized by energy distribution spectra using X-ray microanalysis and the results show that carbon atoms accounted for absolute majority on the surface of absorbents with only a small quantity of other atoms such as oxygen, potassium and iron.

3.4 Evaluation of Natural Gas Adsorption on Carbon Molecular Sieve

Instability in the oil markets and increase in environmental concerns have stimulated research for alternative transportation fuels. One alternative to gasoline is natural gas, which consists primarily of methane (85% ~ 95%) with minor amounts of ethane, other higher hydrocarbons, and carbon dioxide. The advantage of natural gas is that it is cheaper than gasoline and readily available in the world. Natural gas burns more cleanly than gasoline, emitting fewer toxic hydrocarbons and 90% less carbon monoxide. At present, many governments are actively making efforts to popularize natural gas-driven vehicles, mainly driven by compressed natural gas (CNG), in big city to alleviate the pollution caused by exhaust gas.

The use of natural gas as vehicular fuel, an application where storage volume is limited, has necessitated the use of high-pressure storage, which requires high pressure (20 ~ 30MPa) and an expensive multi-stage compression facility, to give an adequate if not entirely satisfactory driving range. Numerous vehicles have been adapted to use compressed natural gas (CNG) as fuel, which is stored in heavy steel cylinders. The net deliverable capacity for CNG at 1.35 atm (5 psi) is 215 standard liter per liter of storage volume. The disadvantages of such high pressures have stimulated research into the use of absorbents in an attempt to provide a similar energy density, but at relatively low pressure (typical target of 3.4 MPa, 500 psi) achievable by single-stage compression. This concept of absorbed natural gas (ANG) can reduce the highest storage pressure so those lightweight cylinders can be used. The key question is whether the net deliverable capacity of such a device can match or exceed that of CNG. Obviously, one needs a high pore volume, high surface area absorbent for this purpose. This kind of novel carbon molecular sieve produced in our laboratory is such material suitable for the application of ANG.

From above data, derived from characterization of the absorbents in previous sections, it is clear that BET surface area varies with other structural parameters, such as average pore size and microporosity, in direct proportion. Therefore, absorbents differing in BET surface area were used to evaluate the natural gas storage capacity on them by two-vessel volumetric method at 293 K and up to 5.0 MPa. Table 4 submits natural gas storage capacity on absorbents at different pressures. As seen from Table 4, with the increase of storage pressure and BET surface area, natural gas storage capacity enhanced obviously. Of interest is that, with the rise of storage pressure from 3 MPa to 5 MPa, the net increased storage capacity on an absorbent with high BET surface area is large than the one with low BET surface area. Under higher pressure, more relatively large pores play a role in natural gas absorption. Absorbents with higher surface area have more large micropores and small mesopores (20~30Å), which contribute more to natural gas absorption under high pressure than low pressure.

4. CONCLUSIONS

- (1) Activated agent ratio, activated temperature and holding time have much influence on the structure of the Carbon Molecular Sieve;
- (2) Coke preoxidation results in the remarkable decrease of mesopore volume;
- (3) A new crystal phase is formed during activation process;
- (4) Increase in pressure from previously suggested 3.4 MPa^[2] to 5.0 MPa, at which relatively larger pores play a role in natural gas absorption, does allow a greater amount of natural gas to be absorptively stored on the absorbents with high surface area.

This kind of carbon molecular sieve can also be used as microwave adsorbent and PSA adsorbent for gas separation. We are extending study to these areas.

ACKNOWLEDGEMENTS

Financial supports by the Sheng-Li oilfield and Young Scientists Award Foundation of Shandong Province and Young Scientists Innovation Foundation of China National Petroleum Corporation are gratefully acknowledged.

REFERENCES

1. Matranga K. R. and Myers A. L. Glandt E. D., *Chem. Eng. Sci.* **1992**, 47, 1569.
2. Quinn D. F. and Macdonald J. A., *Carbon.* **1992**, 30, 1097.

Table 1. Characterization of carbon molecular sieve structure

W_{ACT}/W_{COKE}	S_{BET} (m^2/g)	D (\AA)	D_{micro} (\AA)	V (~20 \AA) cm^3/g	V(20-30 \AA) cm^3/g	V(30 \AA -) cm^3/g
1	909.3	20.748	8.077	0.356	0.040	0.029
2	1173.9	21.173	8.267	0.403	0.131	0.062
3	2273.5	21.048	8.786	0.636	0.428	0.150
5	2859.5	21.501	8.857	0.762	0.604	0.201

*D: average pore diameter D_{micro} : average micropore diameter
 W_{ACT}/W_{COKE} : weight ratio of activator vs. coke

Table 2. Characterization of carbon molecular sieve structure

T (K)	t (min)	S_{BET} (m^2/g)	D (\AA)	D_{micro} (\AA)	V (~20 \AA) cm^3/g	V(20-30 \AA) cm^3/g	V(30 \AA -) cm^3/g
973	120	2257.9	20.311	8.688	0.697	0.212	0.078
1073	60	2859.5	21.501	8.857	0.762	0.604	0.201
1173	60	2304.8	23.602	9.106	0.585	0.675	0.389
1273	1	3734.9	23.620	9.136	0.925	1.121	0.640

*Activating conditions: $W_{ACT}/W_{COKE}=5$, the rate of elevating temperature=10K/min,
 N_2 flow rate=30ml/min T: activating temperature t: retaining time
 D: average pore diameter D_{micro} : average micropore diameter

Table 3. Characterization of carbon molecular sieve structure

	S_{BET} (m^2/g)	D (\AA)	D_{micro} (\AA)	V (~20 \AA) cm^3/g	V(20-30 \AA) cm^3/g	V(30 \AA -) cm^3/g
Untreated	2859.5	21.501	8.857	0.762	0.604	0.201
Preoxidation	2255.8	20.293	8.626	0.667	0.304	0.084

*D: average pore diameter D_{micro} : average micropore diameter

Table 4. Natural gas absorption capacity on carbon molecular sieves with different surface area

S_{BET} (m^2/g)	V/V (3.0MPa)	V/V (4.0MPa)	V/V (5.0MPa)
1634	86.7	115.6	132.9
2069	127.1	144.2	156.7
2745	150.3	179.8	208.3

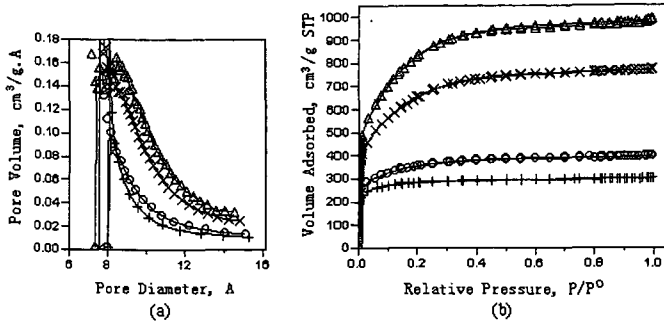


Figure 1. Characterization of carbon molecular sieve structure
 (a): micropore distribution; (b): absorption isotherm

+ : $W_{ACT}/W_{coke}=1:1$; o : $W_{ACT}/W_{coke}=2:1$; x : $W_{ACT}/W_{coke}=3:1$; Δ : $W_{ACT}/W_{coke}=5:1$;

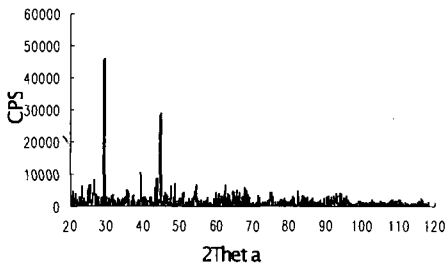


Figure 2. XRD patterns of carbon molecular sieve



(a) Derived from raw coke



(b) Derived from preoxidized coke

Figure 3. The SEM photo of carbon molecular sieves